J Mater Sci (2008) 43:3728–3732
DOI 10.1007/s10853-008-2597-y

LETTER

Deformation micromechanics of spider silk

Victoria L. Brookes · Robert J. Young · Fritz Vollrath

Received: 14 February 2008 / Accepted: 13 March 2008 / Published online: 30 March 2008

The physical and mechanical properties of spider silk have been the subject of analysis and much speculation over the past 40 years [1–8]. Their study has been complicated by the fact that the mechanical properties of these fibres have evolved over evolutionary times and thus respond in a complex way to both external (e.g. temperature and hydration [4]) and internal (e.g. pH environment, extrusion speed [8]) conditions during 'spinning'. However, modern spectroscopic methods are rapidly changing our views of silks and their internal structures. This article sets out to examine the role of Raman Spectroscopy (RS) [6, 7] and the information it provides about the effect of mechanical deformation on the molecular strains and stresses in silks produced at different processing speeds.

Spider dragline silk combines great strength with unmatched elasticity. It has extensions to failure of up to 35% [1, 9] at tensile strengths up to 3 GPa and with moduli up to 10 GPa; all of which compares favourably to the corresponding values for Kevlar 49 of 3%, 3.6 GPa and 130 GPa, or natural rubber of 600%, 0.1 GPa and 0.001 Gpa, respectively [1].

Spider dragline tensile properties vary from species to species and from individual to individual within a species reflecting its use. Thus, different parts of an orb web spun may be spun at different speeds and have different tensile properties [10]. Indeed, with increasing reeling speed spider dragline silk has increased orientation of both crystalline and amorphous fractions [11, 12]. At the same time both the breaking stress and modulus increase whilst breaking strain decreases [8]. Similar effects of spinning rates on silk structure property relations were found for *Bombyx* silkworm silks, suggesting a generic relationship [13].

Raman Spectroscopy has become a key technique to study polymer materials as it is versatile as well as non-destructive. The vibrational analysis it yields provides important information about the chemical and morphological structure of polymers. Thus, not surprisingly, RS has been a key feature of structural studies of silks originating from both spider [14] and silkworm [15–17]. RS has been used as a characterization technique and a tool to study differences in secondary conformation between films, powders and fibres [18–20], the denaturation process [21] and the effect of solvent on fibres [22].

Raman Spectroscopy is a valuable technique for analyzing the mechanical properties of a material because Raman bands shift wavenumber position in response to the application of stress or strain to a sample [23]. The magnitude of this Raman shift depends on the chemical structure and morphology as well as the microstructure of fibres. Young et al. followed both *Bombyx mori* and *Nephila edulis* silk deformation using RS [6, 7]. They found that the 1095 cm^{-1} peak in spider silk and the 1085 cm^{-1} band in silkworm silk each behave in a manner similar to bands in other high performance polymer fibres assigned to the C–C backbone vibrations [24–26]. Further, they also found that the amide III band at approximately 1230 cm^{-1} shifts linearly with stress [6, 7]. This suggests the deformation behaviour to be consistent with a uniform stress model [27]; and that it may be the polypeptide backbone that is the reinforcing unit when the fibre is loaded.

V. L. Brookes · R. J. Young (✉)
Materials Science Centre, School of Materials, University of Manchester, Grosvenor Street, Manchester M1 7HS, UK
e-mail: robert.young@manchester.ac.uk

F. Vollrath
Department of Zoology, University of Oxford, South Parks Road, Oxford OX1 3PS, UK

Previous studies had been concerned only with silk produced under natural spinning conditions. In this present study, we have produced silk with different microstructures and mechanical properties from spiders by spinning at different speeds ranging from 0.5 mms^{-1} to 128 mms^{-1}. This has enabled a systematic study to be made of the effect of fibre structure upon the micromechanics of deformation of spider major ampullate MAA silk.

The *Nephila senegalensis* spiders were reared in controlled conditions in a greenhouse. Webs were sprayed with water every few days, and spiders were fed with flies. The silk samples were obtained from the spiders by natural spinning at around 10 mms^{-1} and by forced reeling at speeds 0.5, 1.9, 10.7, 23.1 and 128 mms^{-1} from fully awake restrained spiders. The major and minor ampullate silk was collected from the spinneret using tweezers and then separated and collected on a motorized bobbin. The diameter of the individual fibres was measured using a Philips Scanning Electron Microscope (FEG-SEM) XL30 system operated at 2 kV.

The mechanical properties of the fibres were determined in controlled conditions of 23 ± 1 °C and 50 ± 5% relative humidity upon individual fibres mounted across cardboard windows using an Instron 1121 universal testing machine fitted with a 10 N load cell. The stress was calculated using the diameter of the fibre determined using the SEM. Raman spectra were obtained using a Renishaw 1000 Raman microprobe system fitted with a near-infrared, 785 nm laser. Spectra were obtained during deformation using the single fibres on cards. These were mounted onto a deformation stress rig that was connected to a transducer for reading the applied load in grams. The fibres were deformed stepwise up to failure by moving the block with the attached micrometer, accurate to within ±0.005 mm. Strain was calculated from the change in fibre length divided by the original gauge length.

The initial Raman deformation experiments were undertaken using *Nephila senegalensis* MAA silk, produced under reeling conditions that mimic natural spinning speeds (Table 1). The Raman band shift of the 1095 cm^{-1} peak is seen in Fig. 1(a) and the dependence of the peak position upon stress is shown in Fig. 1(b). Note that, on stressing these fibres, the band seen at 1095 cm^{-1} shifts position and shows a broadening, which together indicate that local stress distributions occur within the molecules whilst the fibre is being stressed [28].

Silk fibres produced using different reeling speeds were found to have different values of initial Young's modulus as well as different rates of band shift at 1095 cm^{-1} (Table 1). Thus the fibres with the highest level of modulus tended to have the lowest shift rate and vice versa. This observation gives special insight into the micromechanics of fibre deformation. In this context we first consider the

Table 1 Initial fibre modulus and 1095 cm^{-1} Raman band shift rate $d\Delta\nu/d\sigma_f$ as a function of reeling speed

Reeling speed (mms^{-1})	Initial modulus (GPa)	$d\Delta\nu/d\sigma_f$ (cm^{-1} GPa^{-1})
0.5	7.4 ± 0.3	−6.9 ± 0.2
1.9	11.0 ± 0.5	−6.1 ± 2.6
10.7	9.0 ± 0.1	−4.4 ± 0.3
23.1	9.6 ± 0.5	−4.3 ± 0.9
128.6	4.7 ± 1.6	−9.3 ± 2.9
~10[a]	8.4 ± 1.7	−5.0 ± 0.9

[a] Natural spinning speed

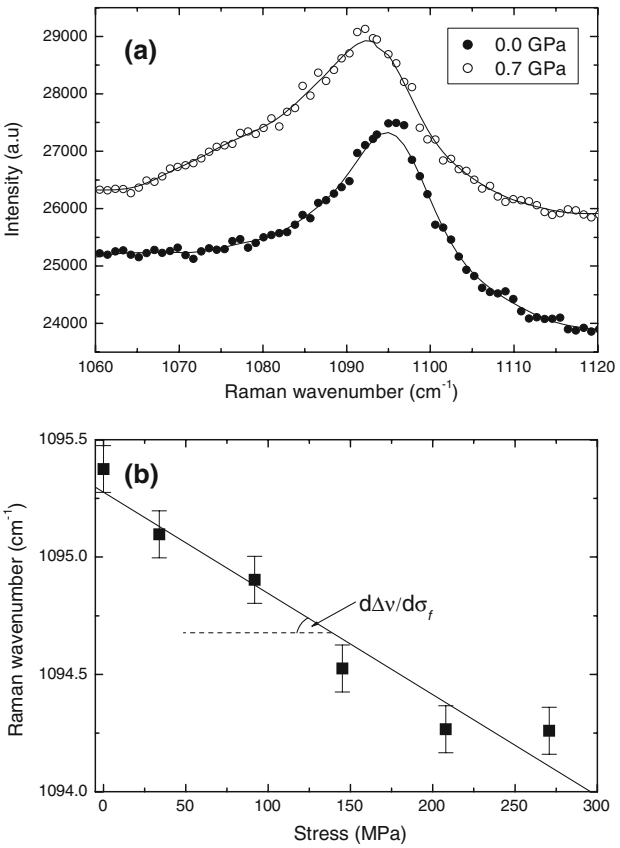

Fig. 1 Behaviour of the 1095 cm^{-1} Raman band of spider silk. (**a**) Shift with stress. (**b**) Dependence of the peak position upon stress

stress-induced Raman bands shifts of conventional high-performance polymer fibres.

High-performance fibres such as PPTA [24–26] and poly(ethylene terephthalate) PET [28, 29] have microstructures in which the stress-bearing units are in series as shown in Fig. 2. The fibres undergo deformation such that the stress on the different units in the fibre microstructure is the same as the overall stress on the fibre. This is known as the *uniform-stress series* model; and it has been suggested [27] that the behaviour of silk fibres follows this model based upon the linearity of the shift of band position against stress (c.f. Fig. 2).

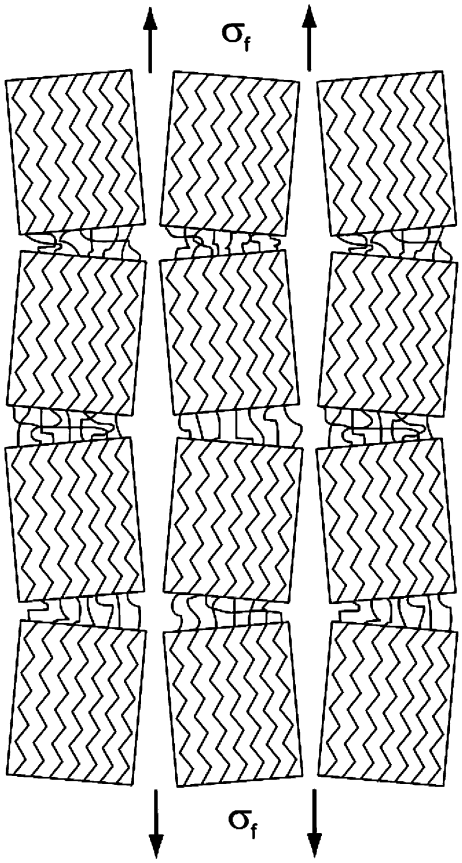

Fig. 2 Schematic representation of the uniform stress series model of the microstructure of a high-performance polymer fibre

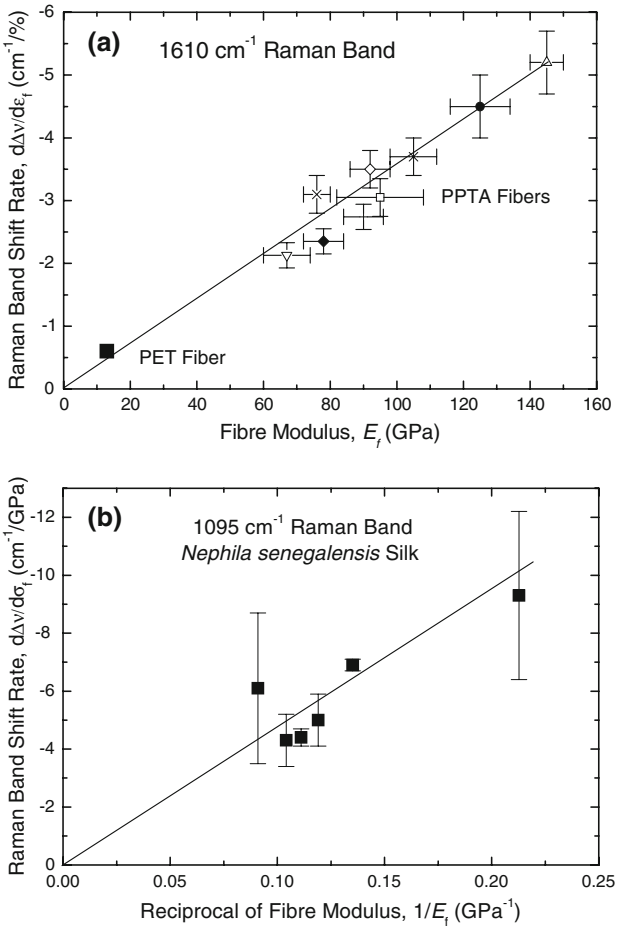

Fig. 3 Raman bands shift rates for different fibres with different microstructures and mechanical properties. (**a**) Shift per unit strain for the 1610 cm^{-1} Raman band of a series of different PPTA and PET fibres [25, 29]. (**b**) Shift per unit stress for the spider silk fibres reeled at different speeds

It appears [23] that the changes in Raman wavenumber, $\Delta\nu$, which take place during the deformation of high-performance fibres, are a result of chain stretching and can be related directly to the stress on the crystalline reinforcing units, σ_r, such that for an increment of stress

$$d\Delta\nu \propto d\sigma_r. \quad (1)$$

Since in this case the stress in the microstructure is uniform then σ_r equals σ_f, the fibre stress, and so Eq. 1 becomes, by dividing by an increment of fibre strain, ε_f

$$\frac{d\Delta\nu}{d\varepsilon_f} \propto \frac{d\sigma_f}{d\varepsilon_f}\,(=E_f), \quad (2)$$

where E_f is the Young's modulus of the fibre. Figure 3(a) shows the dependence of $d\Delta\nu/d\varepsilon_f$ upon fibre modulus for the Raman bands at around 1610 cm^{-1} due to the stretching of the *p*-phenylene groups in a series of PPTA and PET high-performance polymer fibres processed in different ways to give different values of Young's modulus. It can be seen that the data follow the prediction of Eq. 2. As a consequence of this uniform stress series model, the Raman band shift per unit stress, $d\Delta\nu/d\sigma_f$, is constant for the 1610 cm^{-1} band in all fibres containing *p*-phenylene groups in their main chain at around -4.0 cm^{-1}/GPa, regardless of their microstructure and Young's modulus [23].

Inspection of the Raman band shift data for the spider silk fibres in Table 1 shows that $d\Delta\nu/d\sigma_f$ for the Raman band varies with reeling speed, implying that the uniform stress series model (Eq. 2) is not appropriate in the case of the spider silk. This interpretation supports conclusions drawn from *Bombyx mori* fibre deformation analyzed with simultaneous X-ray diffraction [30] showing that crystal modulus varied with the degree of crystallinity of the fibres. In addition, the descriptive model of Termonia [31] for the silk properties is not a uniform stress model.

An alternative composite model that can be employed to model the behaviour of silk is the *uniform strain parallel* model in which the strain on the reinforcing units, ε_r, is the same as the overall fibre strain, ε_f, which leads to

$$\frac{\sigma_r}{E_r} = \frac{\sigma_f}{E_f}, \tag{3}$$

where E_r is the Young's modulus of the reinforcing units. Rearranging and using Eq. 1 gives

$$\frac{d\Delta\nu}{d\sigma_f} \propto \frac{E_r}{E_f}. \tag{4}$$

It can assumed that the modulus of the reinforcement, E_r, is constant, which leads to the prediction [27] that whenever the uniform strain model can be applied to the fibre, $d\Delta\nu/d\sigma_f$ should be proportional to the reciprocal of the fibre modulus, $1/E_f$. Indeed this behaviour is shown in Fig. 3(b) using the data from Table 1 for the 1095 cm^{-1} Raman band, assigned to the C–C backbone in the β-sheets and thought to be the main reinforcing units in the silk structure [31].

A model of the microstructure of the spider silk fibre, consistent with the Termonia model [31] and compatible with the behaviour observed in this study, is shown in Fig. 4. The main feature that sets it apart from the uniform stress model (Fig. 2) is the positioning of the reinforcing units, which here are not lined up in series. This would explain why the stress/strain curves of the spider silk are quite different from those of high-performance fibres, such as PPTA. Silks have a lower Young's modulus while being very much more extensible, which lead to their outstanding levels of toughness [32]. The parallel arrangement of the crystals reduces the Young's modulus of the fibres significantly while allowing the fibres to have much higher levels of extensibility through deformation of the softer amorphous phase. Since the stress on the crystal is not the same as the stress on the amorphous regions, such a structural arrangement would also explain why crystal modulus values determined from simultaneous X-ray diffraction and deformation experiments on different types of silk do not agree well with computed values [30, 33], unlike the results from similar experiments on PPTA [34].

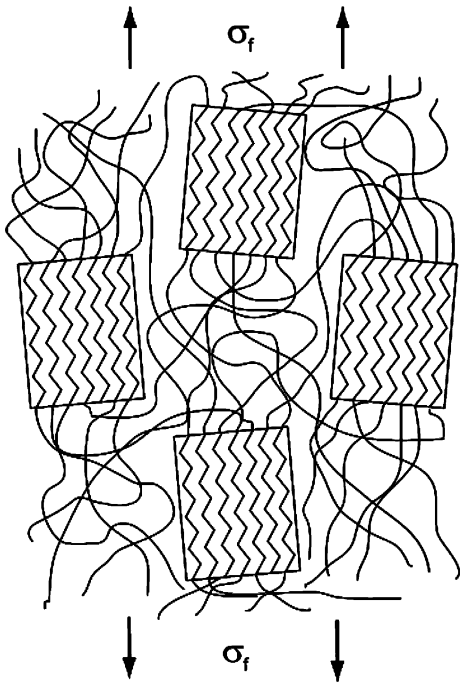

Fig. 4 Schematic diagram of the possible microstructure of spider silk consistent with the uniform strain model

Finally, we must point out that the analysis provided in this article accounts only for the elastic deformation of the material up to the yield stress. The post-yield behaviour is more complex and the strain probably becomes non-uniform leading to features such as band broadening and the band shifts becoming non-linear with stress (Fig. 1).

Previous studies upon stress-induced Raman band shifts suggested that the uniform stress model would be applicable to spider silk. This interpretation was based upon observation that the band shifts of one type of silk were linear when plotted against stress, but not when plotted against strain. This observation alone, however, cannot be sufficient to allow us to distinguish between the different models for the deformation micromechanics of spider silks *in general*. The present study shows that, before the mechanical behaviour can be fully understood, it is necessary to study a range of spider silk fibres—ideally processed in different ways (e.g. by varying reeling speed) in such a way that the fibres have different microstructures and mechanical properties. Only when a model can describe the material in all its breadth, as well as depth, can it be considered comprehensive.

Acknowledgement This work was sponsored by the EPSRC, which also supported one of the authors (VLB) through a research studentship.

References

1. Gosline JM, Demont ME, Denny MW (1986) Endeavour 10:37
2. Grubb DT, Jelinski LW (1997) Macromolecules 30:2860
3. Gosline JM, Denny MW, Demont ME (1984) Nature 309:551
4. Cunniff PM, Fossey SA, Auerbach MA, Song JW (1994) ACS Symposium Series 544:234
5. Kitagawa M, Kitayama T (1997) J Mater Sci 32:2005
6. Sirichasit J, Young RJ, Vollrath F (2000) Polymer 41:1223
7. Sirichaisit J, Brookes VL, Young RJ, Vollrath F (2003) Biomacromolecules 4:387
8. Madsen B, Shao Z, Vollrath F (1999) Int J Biol Macromol 24:301
9. Denny M (1976) J Exp Biol 65:483
10. Perez-Riguero J, Elices M, Llorca J, Viney C (2001) J Appl Polym Sci 82:2245
11. Riekel C, Branden C, Craig C, Ferrero C, Heidelbach F, Muller M (1999) Int J Biol Macromol 24:179
12. Riekel C, Vollrath F (2001) Int J Biol Macromol 29:203
13. Shao Z, Vollrath F (2002) Nature 418:741

14. Shao Z, Vollrath F, Sirichaisit J, Young RJ (1999) Polymer 40:2493
15. Rousseau ME, Lefevre T, Beaulieu L, Asakura T, Pezolet M (2004) Biomacromolecules 5:2247
16. Monti P, Taddei P, Freddi G, Asakura T, Tsukada M (2001) J Raman Spec 32:103
17. Edwards HGM, Farwell DW (1995) J Raman Spec 26:901
18. Tsukada M, Freddi G, Monti P, Bertoluzza A, Kasai N (1995) J Polym Sci Part B: Polym Phys 33:1995
19. Monti P, Freddi G, Bertoluzza A, Kasai N, Tsukada M (1998) J Raman Spec 29:297
20. Gillespie DB, Viney C, Yager P (1994) ACS Symposium Series 544:155
21. Zheng SD, Li GX, Yao WH, Yu TY (1989) Appl Spectros 43:1269
22. Shao Z, Young RJ, Vollrath F (1999) Int J Biol Macromol 24:295
23. Young RJ (1995) J Text Inst 86:360
24. van der Zwaag S, Northolt MG, Young RJ, Robinson IM, Galiotis C, Batchelder DN (1987) Polym Comm 28:276
25. Young RJ, Lu D, Day RJ, Knoff WF, Davis HA (1992) J Mater Sci 27:5431
26. Young RJ, Lu D, Day RJ (1991) Polym Intl 24:71
27. Young RJ, Eichhorn SJ (2007) Polymer 48:2
28. Yeh WY, Young RJ (1999) Polymer 40:857
29. Yeh WY, Young RJ (1994) Polymer 35:3844
30. Sinsawat A, Putthanarat S, Magoshi Y, Pachter R, Eby RK (2002) Polymer 43:1323
31. Termonia Y (1994) Macromolecules 27:7378
32. Vollrath F, Porter D (2006) Appl Phys A 82:205
33. Nishino T, Nakamae K, Takashi Y (1992) Polymer 33:1328
34. Montes-Morán MA, Davies RJ, Riekel C, Young RJ (2002) Polymer 43:5219